RESEARCH PAPER

The variable external magnetic field effect on corrosion behavior of drilling casing of oil and gas wells in matrix acidizing with HCl solution: Experimental study and modelling

Abbas Hashemizadeh[1,*], Mohammad Javad Ameri[2], Babak Aminshahidy[3], Mostafa Gholizadeh[4]

[1] *Chemical Engineering Department, Faculty of Engineering, University of Qom, Qom, Iran.*

[2] *Petroleum Engineering Department, Amirkabir University of Iran, Tehran, Iran.*

[3] *Oil And Gas Research Institute, Ferdowsi University of Mashhad, Mashhad, Iran.*

[4] *Department of Chemistry, Faculty of Science, Ferdowsi University of Mashhad, Mashhad, Iran.*

ARTICLE INFO

Article History:
Received 18 May 2021
Revised 08 September 2021
Accepted 10 September 2021

Keywords:
HCl Acidizing,
Drilling Casing,
Corrosion rate,
Modelling,
Response surface methodology

ABSTRACT

The magnetic field (MF) affects the corrosion rate of N-80 carbon steel (which is frequently used in petroleum industry) in 3.8 Molar (or 12.5% weight percent). HCl was studied first at different conditions by implementing the potentiodynamic polarization (PDP) and gravimetric weight loss (WL) procedures. Response Surface Methodology (RSM) was next implemented to investigate and simulate the impacts of intensity of the magnetic field, time of magnetization, and elapsed time on the efficiency of corrosion inhibition (η). The test results revealed that acid magnetization considerebly decreases the rate of corrosion of N-80 carbon steel (CS) in the presence of HCl up to 93% so that it can be used as an eco-friendly and cost-effective substitute for the common corrosion inhibitors. The results also revealed that η enhances by enhancing the intensity of magnetic field. The morphology of the N-80 CS surface was also studied using SEM in the magnetized and normal HCl solutions.

How to cite this article
Hashemizadeh A., Ameri MJ., Aminshahidy B, Gholizadeh M, The variable external magnetic field effect on corrosion behavior of drilling casing of oil and gas wells in matrix acidizing with HCl solution: Experimental study and modelling, Journal of Oil, Gas and Petrochemical Technology, 2021; 8(2): 1-13. DOI:10.22034/jogpt.2021.269918.1090.

1. INTRODUCTION

Because of the accessibility and high-dissolving susceptibility of rock, HCl solution has been implemented as the central stimulation liquid in the petroleum industry like oil well acidizing [1]. Despite the frequent usage, the high rate of corrosion of HCl with steels makes several technical issues in practice [2]. The corrosion inhibitors lend themselves to delayed rates of reaction, and small corrosivity [3–6]. However, the challenge of injection issues still exists with additives because of the increasing acid viscosity [7].

The change in the structure and properties of materials during the magnetic field (MF) exposeure is a significant issue in different applications [8–12]. It has been stated that magnetized water causes several phenomena such as the reduction of the rate of carbon steel corrosion in water [13], decreasing rate of corrosion of AISI316L SS in Ringer's solution [14], and reducing corrosion in the aqueous solution of NaC1 [15,16]. Test results revealed that used magnetic fields can influence the corrosion rate of metals or alloys in the aqueous solutions [16–21]. Sagawa showed that iron and copper corrosion in nitric acid

* *Corresponding Author Email: a.hashemizadeh@hsu.ac.ir*

decreased by a constant magnetic field [22]. A rate of corrosion reduction in the surface of the electrode with a great density of the magnetic flux was identified. This reduction rate of dissolution is considerably higher in the existence of chloride ions [23]. The rate of pure iron corrosion in chloride and sulphate solutions has also been observed to significantly reduce under the effect of the magnetic field [24]. The corrosion decreases the impact of a perpendicular magnetic field on AISI 303 stainless steel corrosion in solution with Fe^{3+}, which is a corrosion agent [25]. The magnetic field decreased the steel dissolution in sulphuric acid in which the influence was higher at the lower presence of acid and in the absence of the inhibitor [26]. Also, the avoiding impact of the magnetic field on brass, zinc and aluminium corrosion has been studied [27].

To the best knowledge of the author, no investigation has ever explored the impact of magnetization on the N-80 CS rate of corrosion in HCl solution. All of the past studies faced an external magnetic field that was implemented on the reaction cell; however, the fluid magnetization before coming in contact with N-80 CS was studied. In the this study, the effect of magnetic field on the efficiency of the corrosion inhibition (η) of N-80 CS (that is one of the most conventional materials in the petroleum industry [28]) in HCl was demonstrated by the potentiodynamic polarization (PDP) and gravimetric weight loss (WL) procedures. The influence of the intensity of the magnetic field, elapsed time, and time of magnetization were confirmed in 13 tests. Tests were performed using the design of experiments method through Box-Behnken RSM (Response Surface Methodology) design. Last, the dependence of η on the variable factors was specified in the model. Because of the efficacious magnetization performance on decreasing the rate of corrosion, it was found that the magnetized HCl is an eco-friendly and cost-effective alternative for the regular HCl.

2. EXPERIMENTAL METHOD

2.1. Magnetizer procedure

Various kinds of magnetic devices can be based on the electromagnets (yoke-based and solenoids electromagnets) or permanent magnets. Though electromagnets can create high-intensity magnetic fields, their usage is not functional, since they require an electrical power supply, regular services, and cooling. The existing materials with permanent magnetization such as the rare earth alloys, ferrite, and alnico create fields with appropriate intensity. There are numerous magnetic systems which are implemented for the magnetized liquids production. The magnetic field can be perpendicular or parallel with the direction of flow (Fig. 1) [29].

In this paper, the permanent MF influence on the intense HCl solution (12.5% weight in water or 3.8 M respectively) was obtained. The tests were done by the circulation system presented in Fig. 2. Plastic fittings were implemented to make a connection between the magnetic circuit and the pump, which was connected to the flow meter.

2.2. Electrochemical Measurement

Electrochemical and corrosion experiments were done by an IVIUM potentiostat (IVIUM Technologies, USA) which used a USB cable and a common 3-electrode cell to connect to a computer. The electrochemical cell includes a 3-electrode system. The utilized API N-80 grade electrode was one of the best conventional materials in

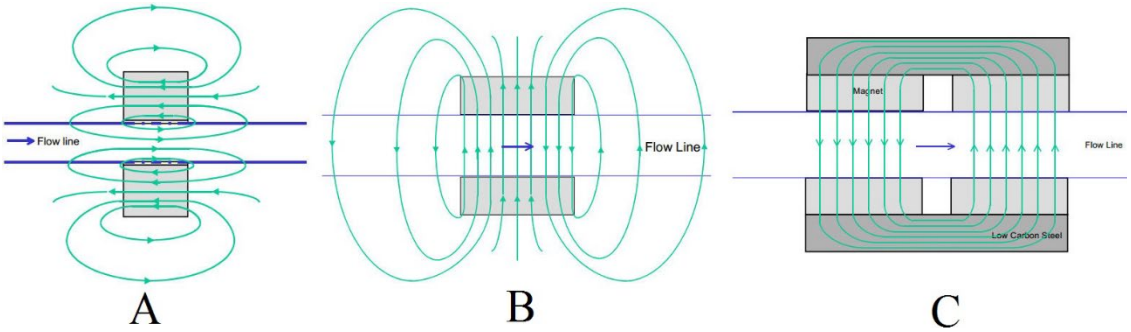

Figure 1: Orientation of the magnetic field (A) using a ring magnet in open circuit (B) using two cylindrical magnets in open circuit (C) using four block magnets in closed circuit.

the petroleum industry [28] with a surface area equal to 1.08 cm^2 and isolated in a glass tube by a thin epoxy resin layer, putting just the end part of the rod in contact with the solution. Before any inspection, this electrode was polished to a mirror-like finish. The N-80 carbon steel electrode was situated horizontally. The reference electrodes and counter were AgAgCl3 saturated calomel electrodes (SCE) and platinum rod, respectively. The potentials of the electrode were recorded during the test and presented here regarding SCE. The working electrode was firstly submerged into the solution for 10-30 minutes until a S.S. of OCP (open circuit potential) reached (without stirring). The curves for the potentiodynamic polarization were plotted at a scan rate of 1.0 mV/s and in the potential limit from −250 to +300 mV versus the OCP. All the electrochemical experiments were conducted in room condition at 308 K. Each measurement was conducted at least 3 times and the obtained data points were presented in the figs and tables to ensure their appropriate reproducibility.

2.3. Measurement of corrosion weight loss

The magnetic emery paper was used to abrade the N-80 CS rectangular 6.28 cm × 1.80 cm × 0.37 cm samples. The samples were then weighed by digital scale (±0.1 mg), submerged in glass beakers including 100 ml 12.5 wt.% (3.8 M) magnetized and normal HCl. In each experiment, the suitable HCl was poured into a fluid magnetizer setup as presented in Fig. 2 and circulated for a specific time to prepare the magnetized acid. A water thermostat bath was utilized to keep the temperature at 21 ± 0.1 C. After 6 hours, the samples were removed, rinsed with water, dried with tissue paper, and weighed again with the high precision.

2.4. Design of Experiments

Regarding the influencing factors in the fluid magnetization, 3 parameters were chosen for this test which included the intensity of the magnetic field, time of the magnetization, and the elapsed time at 3 various stages (Table 1).

The response surface methodology was implemented as a systematic design of experiments (DOEs) procedure. The response surface procedure (RSM) is a method designed to reach the effective factors on the finest response value[30]. It was effectively implemented in the empirical studies [31–33]. The maximum number of the factorial experiments of 27 (3^3) can be finished in only 13 runs (see Table 2), which involve numerous experiments, that are substantial in both the experimental time and cost. Then, RSM including Box-Behnken design and the regression analysis

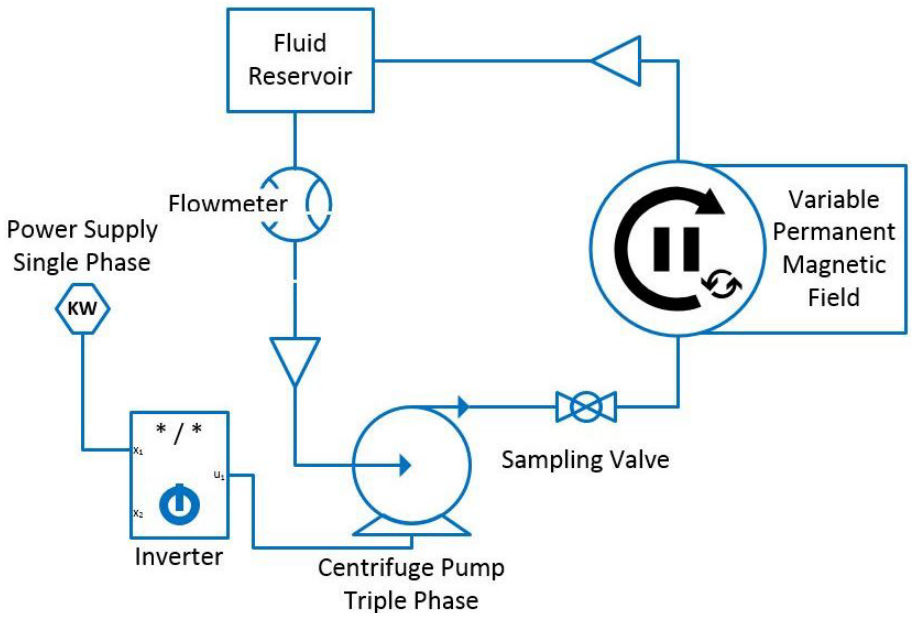

Figure 2: Schematic of experimental setup of fluid magnetizer

Table 1: Three factors and three levels selected in the DoE study of the magnetized HCl

Factor	Factor Description	Levels		
		1	2	3
X_1	Magnetic field intensity (Gauss)	0	2500	5000
X_2	Magnetization time (Minute)	4	6	8
X_3	Elapsed time (Hours)	0	24	48

Table 2: Factors and levels for Box-Behnken study.

Trial	Factor		
	X_1: Magnetic Field Intensity (Gauss)	X_2: Magnetization Time (Min)	X_3: Elapsed Time (Hours)
T1	0	4	24
T2	5000	4	24
T3	0	8	24
T4	5000	8	24
T5	0	6	0
T6	5000	6	0
T7	0	6	48
T8	5000	6	48
T9	2500	4	0
T10	2500	8	0
T11	2500	4	48
T12	2500	8	48
T13	2500	6	24

were implemented to improve the empirical model for η because of the acid magnetization. Based on this model, the response optimization (corrosion rate reduction) was performed.

2.5. SEM surface analysis

The SEM imaging was used to determine the morphologies of N-80 CS sample surfaces after submerging in 3.8 Molar magnetized and normal HCl solution for 6 hours.

3. RESULTS AND DISCUSSION

3.1. Weight loss study

The rate of corrosion (ν) was obtained from the next equation [34]:

$$\nu = \frac{W}{St} \quad (1)$$

Where W= weight loss (g), S= entire area of one sample (m^2), and t= time of the immersion (h). With the obtained rate of corrosion, the corrosion reduction rate (η) was obtained as below [34]:

$$\eta = \frac{\nu_0 - \nu}{\nu_0} \times 100\% \quad (2)$$

Where ν_0 and ν are the rates of corrosion in the magnetized and normal HCl, respectively.

The iron corrosion electrochemical reaction includes the relocation of 2 electrons, then there are 2 levels (ν_s = 2) which each presents the transfer of 1 electron, one of those will be regarded as the level that determines the rate [35]. The recommended iron reaction in the solutions including Cl^- ions are as below [36,37]:

$$Fe + H_2O + Cl^- \Leftrightarrow [FeClOH]^-_{ads} + H^+ \quad (3a)$$

$$[FeClOH]^-_{ads} \Leftrightarrow [FeClOH]_{ads} + e^- \quad (3b)$$

$$[FeClOH]_{ads} + H^+ \Leftrightarrow Fe^{2+} + Cl^- + H_2O \quad (3c)$$

Investigations of the potential of the steel corrosion ($E_{corr.}$) values in HCl, represent that the polarization happens frequently at the anode [35,38,39]. Consequently, the rate of the corrosion reduction of the magnetized HCl (as presented in Table 3) can be clarified based on the activity of Cl^- ion and its influence on the metal dissolution acceleration [36].

Materials will have a different molecular form because of the magnetization [40]. Many researchers who studied the magnetic field impacts on the hydrogen-covered structure, observed an enhancement in the number of the

Table 3. Changes in the corrosion rate of CS in HCl due to the magnetization of HCl

Trail	Combination of Factors	WL of CS in Normal HCl (g)	WL of CS in Magnetized HCl (g)	CR of CS in Normal HCl (g/cm²h)	CR of CS in Magnetized HCl (g/cm²h)	Corrosion Inhibition Efficiency (%)
T1	$X_{11}X_{21}X_{32}$	0.3219	0.3219	0.00183	0.00183	0
T2	$X_{13}X_{21}X_{32}$	0.3219	0.0728	0.00183	0.00044	76.17
T3	$X_{11}X_{23}X_{32}$	0.3219	0.3219	0.00183	0.00183	0
T4	$X_{13}X_{23}X_{32}$	0.3219	0.0525	0.00183	0.00031	82.81
T5	$X_{11}X_{22}X_{31}$	0.3219	0.3219	0.00183	0.00183	0
T6	$X_{13}X_{22}X_{31}$	0.3219	0.0433	0.00183	0.00026	85.84
T7	$X_{11}X_{22}X_{33}$	0.3219	0.3219	0.00183	0.00183	0
T8	$X_{13}X_{22}X_{33}$	0.3219	0.0471	0.00183	0.00028	84.64
T9	$X_{12}X_{21}X_{31}$	0.3219	0.0195	0.00183	0.00012	93.48
T10	$X_{12}X_{23}X_{31}$	0.3219	0.0537	0.00183	0.00032	82.47
T11	$X_{12}X_{21}X_{33}$	0.3219	0.0654	0.00183	0.00048	73.73
T12	$X_{12}X_{23}X_{33}$	0.3219	0.0736	0.00183	0.00038	79.17
T13	$X_{12}X_{22}X_{32}$	0.3219	0.0530	0.00183	0.00032	82.71

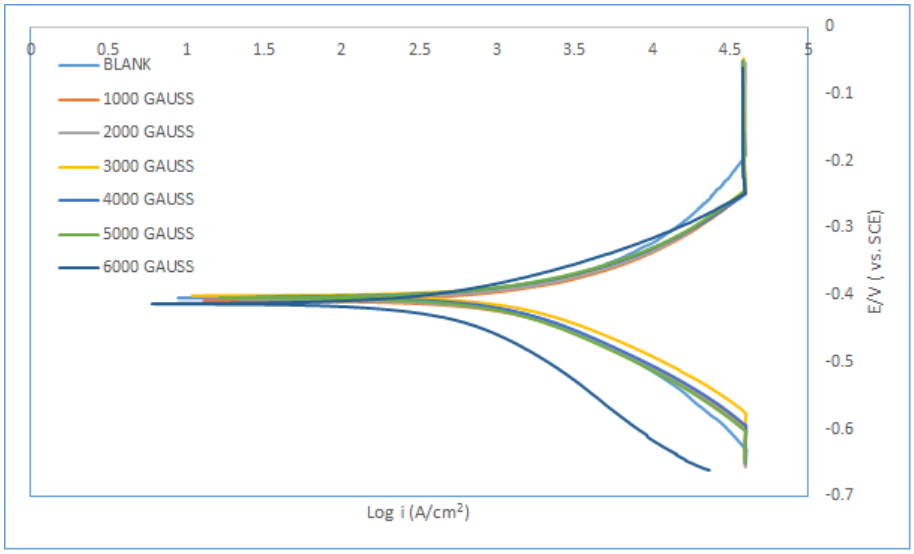

Figure 3: Potentiodynamic polarization curves of N-80 CS in normal and magnetized 3.8 M HCl solution (scan rate 1 mVs_1).

hydrogen bonds [41–43]. It is also recommended that the hydrogen-covered intensity increased by 10 Tesla under the magnetic field in the hydrogen-covered molecules [44]. Enhancing hydrogen bond strength and their number decreases the choler molecules' activity and may decrease the corrosion rate of HCl. The results of the current study are consistent with those carried out on the rate of AISI316L SS corrosion in Ringer's solution, rate of steel corrosion in water, and the aluminum corrosion in aqueous NaC1 solution in a magnetic field [13–15], and other related tests [22–27].

Moreover studies on the impact of the magnetic fields on the electrochemical reactions have shown that these impacts became stronger as the water conductivity is enhanced by ionic solutes [45,46]. They found that this would tend to decrease any ions or anomalous pH values concentrations and could therefore minimize the localized corrosion impacts [45–48].

3.2. Potentidynamic polarization study

Potentiodynamic polarization curves are documented and presented in Fig. 3 to attain information about the magnetization effect on the electrochemical corrosion behavior of N-80 CS

Table 4. Electrochemical parameters of N-80 CS in 3.8 M HCl solution under various magnetic fields at room temperature.

Magnetization	E_{corr} (mV)	ba (mV/dec)	bc (mV/dec)	I_{corr} (μA/cm^2)	CRR (%)
Blank	-405.9	50	69	756.1	---
1000 Gauss	-412.2	40	54	502.6	33
2000 Gauss	-406.9	33	49	499.1	34
3000 Gauss	-406.9	33	50	489.7	35
4000 Gauss	-405.1	29	46	437.2	42
5000 Gauss	-406.8	30	47	410.3	46
6000 Gauss	-469.8	69	58	87.8	88

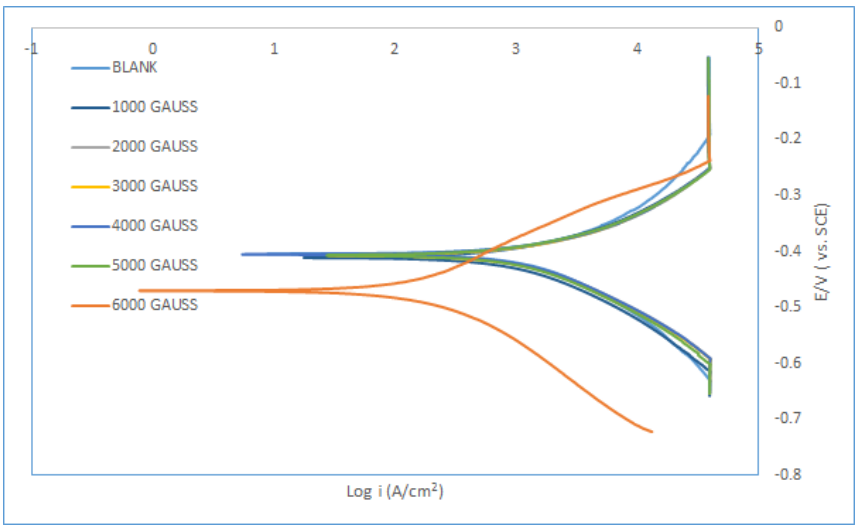

Figure 4: Potentiodynamic polarization curves of N-80 CS in normal and magnetized 3.8 M HCl solution (scan rate 1 mV s_1) after 24 hours.

in 3.8 M HCl solution under numerous magnetic fields. Related electrochemical kinetic parameters like the potential of corrosion (E_{corr}), corrosion current density (i_{corr}) and cathodic Tafel slope (b_c), obtained from these tests, are shown in Table 4. The efficiency of the corrosion inhibition (η) because of solutions, so the magnetization is obtained by:

$$\eta = \frac{i_{corr} - i'_{corr}}{i_{corr}} \quad (4)$$

Where i'_{corr} and i_{corr} = densities of corrosion current for N-80 carbon steel electrode in the magnetized and normal solutions, respectively.

As it can be observed in Fig. 3, the anodic branch of the potantiodynamic polarization curve is unpretentious by various MFs that is related to studies in literature [47,49–53]. The influence of the magnetic fields in the earlier studies on the iron passivation revealed that the magnetic fields have slight on the iron passivation monitored by the electron-transfer level, but the passivation is monitored partially by mass transfer step (MTS). Though, MF changes the active–passive transition states [47,51,54]. The mass transport control was a central parameter in dissolution at small overpotentials in anodic and cathodic reactions (nearly 20 mV). $Fe(OH)_2$ formation on the surface of iron is a significant factor to the resistant corrosion and plays a key role in the reduction of dissolution [21–24]. The cathodic hydrogen ion decrease influenced by MF on potantiodynamic polarization curve enhanced that was defined by anodic shift of E_{corr} [17]. As observed in the Fig. 3, the MF suppressed the reduction rate of hydrogen which is the reduction rate of hydrogen in the used MF solution and led to reduce the corrosion current density. The corrosion current density reduced by enhancing the MF (Table 4). The happening might be related to enhance the $Fe(OH)_2$ formation as a barrier covering the surface of iron and decrease the corrosion current density an enhanced η

up to 92%. Fig. 4 shows that 24 hr after exposing HCl to the MF, the effect of magnetization stay in the acid. By enhancing the MF, the impact of magnetization remains for longer time (Table 5). This way could be defined by the Lorentz force driven convection [55].

3.3. Analysis of Variance (ANOVA)

The tests were carried out randomly for the minor unrestrained impact of the factors. A quadratic polynomial equation was established for forecasting the responses as independent variables including the squared terms and quadratic interactions. Eq. (6) presents the basis of creating a polynomial equation:

$$Y = \beta_0 + \sum_{j=1}^{3}\beta_j X_j + \sum_{j=1}^{3}\beta_{jj} X_j^2 + \sum_{i<j}^{3}\beta_{ij} X_i X_j + \sum_{i<j<k}^{3}\beta_{ijk} X_i X_j X_k \quad (5)$$

Several regression analysis methods included in the RSM were implemented to approximate the coefficients of the models. Equation (7) presents the second-order models that were used to reduce the rate of corrosion:

$$\eta = 5.90875 + 0.047624\mathrm{X}_1 + 2.23938\mathrm{X}_2 - 0.72693X_3 + 3.320\times10^{-4}X_1X_2 - 5\times10^{-6}X_1X_3 + 0.085677X_2X_3 - 6.60460\times10^{-6}X_1^2 - 0.42156X_2^2 + 2.06380\times10^{-3}X_3^2 \quad (6)$$

One statistical method is the analysis of variance (ANOVA) whose main purpose is to find the extent of variation of each factor from the results and leads to the entire variation detected in the results [56]. Fundamentally, it calculates the parameters of the sum of squares (*SSQ*), variance (*V*), degree of freedom (*DF*), F-value, and the contribution percentage for each factor [57]. The F value is the mean square ratio of regression to the error mean square. Provided that in a certain probability level (e.g., $F_{0.05}(9,3)=8.81$), the F value table is smaller than the obtained F-value, a statistically important factor or relationship is achieved. The results of ANOVA presented in Table 6 show the F value of 66.57 for the model. This value is greater than the F table of 8.81 and approves the high significance of the model. The P-value less than 0.05 displays the significance of the factor at 95% confidence limit. The error and the mean square calculations of the model are:

$$MS_{model} = \frac{ss_{model}}{df_{model}} \quad (7)$$

$$MS_{error} = \frac{ss_{error}}{df_{error}} \quad (8)$$

Where SS, df, and MS are the sum of squares, degree of freedom, and mean squares, respectively. The F value obtained by the next Eq:

$$F = \frac{MS_{model}}{MS_{error}} \quad (9)$$

Table 5. Electrochemical parameters of N-80 CS in 3.8 M HCl solution under various magnetic fields at room temperature after 24 hours.

Magnetization	E_{corr} (mV)	ba (mV/dec)	bc (mV/dec)	I_{corr} (μA/cm^2)	CRR (%)
Blank	-405.9	50	69	756.1	---
1000 Gauss	-409.8	37	53	570.1	25
2000 Gauss	-408.4	38	54	573.7	25
3000 Gauss	-400.9	32	45	516.0	32
4000 Gauss	-403.7	35	52	516.4	32
5000 Gauss	-404.8	33	51	438.4	42
6000 Gauss	-412.1	32	63	196.9	74

Table 6: Analysis of variance (ANOVA) for the determination of significant factors which influence CR due to HCl magnetization

Factor	Degree of Freedom	Sum of Squares	Mean Square	F-Ratio	P-Value	R^2
Model	9	18942.43	2104.71	66.57	0.0027	0.9950
Residual	3	94.84	31.61			
Total	12	19037.28				

High R^2 values for Eq. (6) show a suitable fitting for the test data and the anticipated values. Fig. 5a shows the detected in relation to the anticipated values. According to this figure, the greatest values of the test points are located near the straight line that are the anticipated values. The linearity of the pattern also displays that there is no need for the change in the response. Fig. 5b shows the residuals against the test run order. It shows the lurking variables that might have affected the results during the test. The scheme displays a random scatter that brings assurance against the trends ruining the analysis.

3.4. Response Surface Plots and Contour Plots

Eq. (6) was implemented to set up the contour plots and the response surface. These schemes simplify a clear comparison of the dependent variable on the main procedure variables. Figs. 6-8 display response surface schemes of the η (%) as a design variable magnetized HCl. In addition to the central impacts, the interaction impacts between the parameters are clarified. These figures are on the basis of keeping the third variable at the best values. The η considerably improved by increasing the intensity of the magnetic field and reduced with the passage of time.

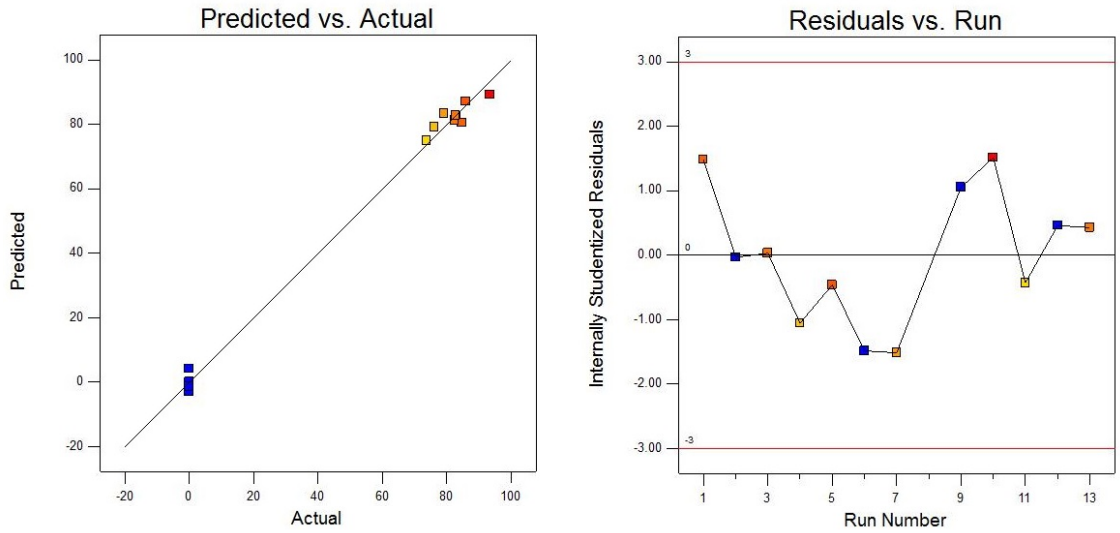

Figure 5: (a) Normal plot of residuals; (b) Residuals of each run.

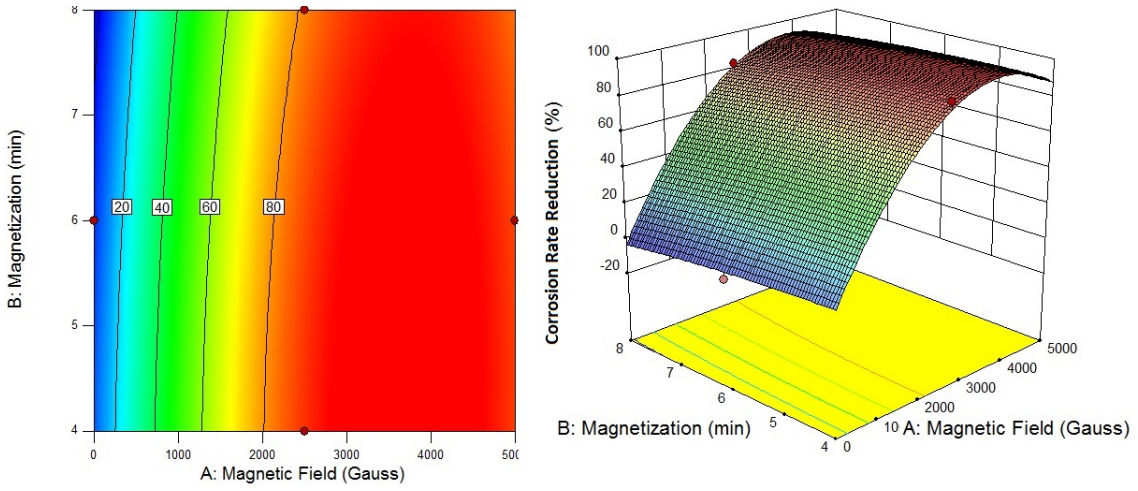

Figure 6: Corrosion rate reduction (η) response surface plot and contour-lines map depending on magnetic field intensity (Gauss) and magnetization time (min), holding third variable at fixed level (elapsed time=0 hr) in 3.8 M. HCl at 21℃

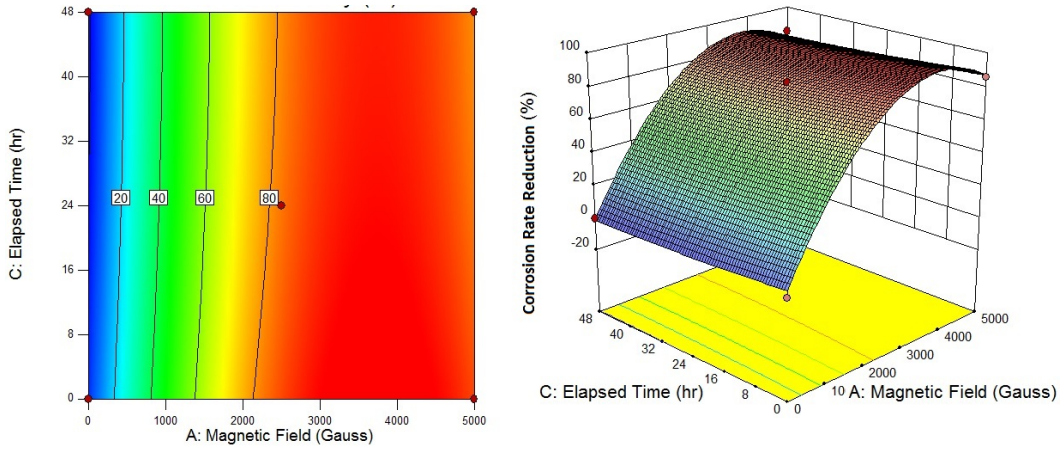

Figure 7: Corrosion rate reduction (η) response surface plot and contour-lines map depending on the magnetic field intensity (Gauss) and the elapsed time (hr), holding third variable at the fixed level (magnetization time=6 min) in 3.8 M % HCl at 21°C

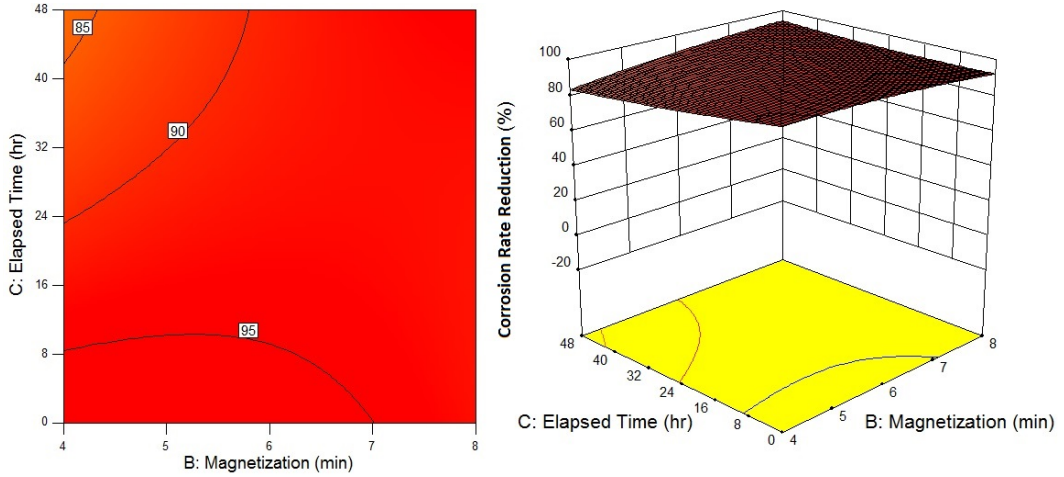

Figure 8: Corrosion rate reduction (η) response surface plot and contour-lines map depending on magnetization time (min) and elapsed time (hr), holding third variable at fixed level (magnetic field=4000 Gauss) in 3.8 M HCl at 21°C

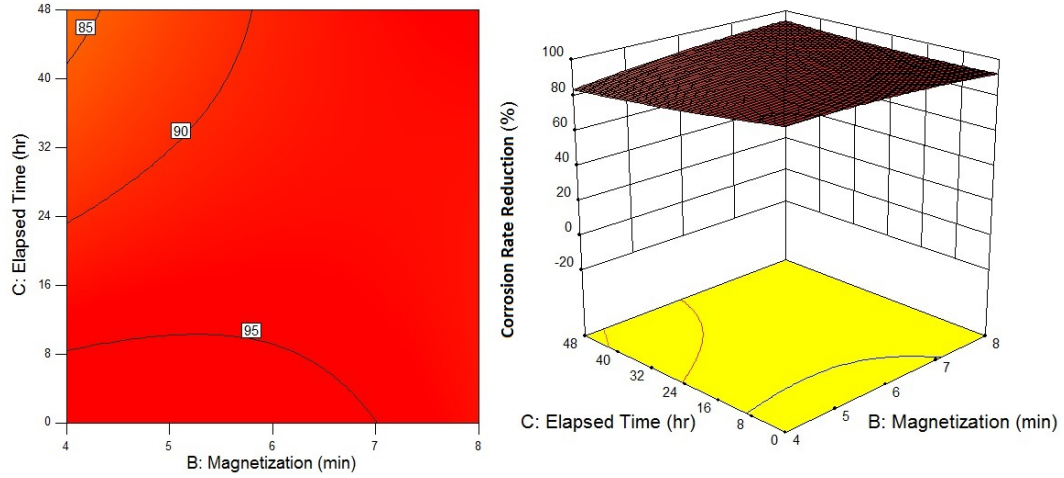

Figure 9: SEM images for (a) unexposed carbon steel; (b) exposed carbon steel in 12.5 wt.% normal HCl solution, and (c) exposed carbon steel in 12.5 wt.% magnetized HCl solution after 6 h immersion at 294 K.

We see a rapid enhance in η by increasing the intensity of MF from 0.0 to 4000 Gauss that was anticipated. This value is greater on the first step of the elapsed time (=0 h). It is allocated to the magnetization that improves the hydrogen bonds, that is acid resistant and reduces the rate of corrosion [13–15]. In other words, as shown in Fig. 6, by enhancing the intensity of the magnetic field, the concentration of [H+] in HCl and as a result its corrosion rate caused by the magnetization reduces. An additional explanation is that when acid passes a magnetic field, its molecular formation will be affected and it becomes more ordered [40], so the movement of molecules will be controlled and the rate of the reaction with N-80 CS decreases.

Fig. 7 demonstrates that enhancing the time of magnetization of flowing liquid in MF from level 1 to level 3, does not highly change the η . Regarding the Lorentz force, when a particle with charge q passes from a magnetic field B with velocity v, then it experiences a force namely Lorentz force [58–60]. This force relies on time, yields legal results, and shows that the magnetic field changes the liquid at the first moments. However, the magnetization period might affect the liquid magnetic memory in which it can keep its magnetic features in a wide interval.

Figs. 8 displays the response surface diagrams and counterplots of η for the magnetized acid. The decrease in the rate of corrosion reduces slightly over the time. The results show that the magnetized acid keeps 80% of its feature in the initial 48 hr from the production. The initial 24 hr is the finest time for the inhibition effciency.

3.5. Surface morphological results and analysis

SEM was used to investigate the CS surface morphologies exposed and unexposed to the magnetized and submerged in normal HCl for 6 h at 294K. Prior to contact with the corrosive solution, the parallel properties were determined on the clean surface of the polished N80 CS that are related to polishing scratches (Fig. 9a). Micrographs analysis in Fig. 9 show that the CS sample displays a quite rough surface in normal (un-magnetized) HCl. As estimated owing to acid solution corrosive attack, normal HCl destructed the surface of CS severely (Fig. 9b). The SEM results were also implemented to the surface of CS after the magnetized HCl exposure (Fig. 9c) which shows that the surface is relatively softer than in the normal HCl and reveals the inhibiting influence of the magnetization.

4. CONCLUSION

The corrosion inhibition effectiveness of the magnetized 12.5 wt.% (3.8 M) HCl with N-80 CS was studied by the potentiodynamic polarization (PDP) and weight loss (WL) methods and was modelled using RSM. The following results could be emphasised:

- The attained results show that, HCl pre-magnetization makes outstanding N-80 CS corrosion rate reducer in 12.5 wt.% (3.8 M) HCl solution.
- ANOVA results showed that the key parameter influencing the efficiency of the corrosion inhibition (η) is the intensity of the magnetic field (MF) with about 71% of participation. However, the effect of the elapsed time is also substantial. The influence of time of the magnetization is insignificant and negligible.
- The efficiency of the corrosion inhibition was observed about 94% for the magnetized HCl (12.5 wt.%) in a 2500 Gauss magnetic field. It enhances by the magnetic field intensity but reduces over time.
- The soft surfaces found in magnetized HCl SEM micrographs reveals that it efficiently keeps N-80 CS against corrosion.
- Because of the corrosion rate reduction during the magnetization process, it is suggested that it can magnetize acid and, in this way, it can be a reliable and cheap substitute for the retarder acids in acidizing the matrix of oil and gas wells.

REFERENCES

[1] McLeod, H. O. Matrix Acidizing. *J. Pet. Technol.* **1984**, *36* (12), 2, 52–55, 69.

[2] Avdeev, Y. G.; Kuznetsov, Y. I.; Buryak, A. K. Inhibition of Steel Corrosion by Unsaturated Aldehydes in Solutions of Mineral Acids. *Corros. Sci.* **2013**, *69* (Supplement C), 50–60.

[3] Atta, A. M.; Elsockary, M. A.; Kandil, O. F.; Shaker, N. O. Nonionic Surfactants from Recycled Poly(Ethylene Terephthalate) as Corrosion Inhibitors of Steel in 1 M HCl. *J. Dispers. Sci. Technol.* **2008**, *29* (1), 27–39.

[4] Al-Sabagh, A. M.; Elsabee, M.; Elazabawy, O. E.; El-Tabey, A. E. Corrosion Inhibition Efficiency of Polytriethanolamine Surfactants for Pipe-Lines Carbon Steel in 1M HCl. *J. Dispers. Sci. Technol.* **2010**, *31* (10), 1288–1297.

[5] Mobin, M.; Aslam, J.; Al-Lohedan, H. A. Study on the Inhibition of Mild Steel Corrosion by Cationic Gemini Surfactant in 1 M HCl. *J. Dispers. Sci. Technol.* **2016**, *37* (7), 1002–1009.

[6] Al-Shafey, H. I.; El Azabawy, O. E.; Ismail, E. A. Ethoxylated

Melamine as Corrosion Inhibitor for Carbon Steel in 1M HCl. *J. Dispers. Sci. Technol.* **2011**, *32* (7), 995–1001.
[7] Ji, Q.; Zhou, L.; Nasr-El-Din, H. Acidizing Sandstone Reservoirs With Aluminum-Based Retarded Mud Acid. *SPE J.* **2015**.
[8] Zakinyan, A.; Dikansky, Y.; Bedzhanyan, M. Electrical Properties of Chain Microstructure Magnetic Emulsions in Magnetic Field. *J. Dispers. Sci. Technol.* **2014**, *35* (1), 111–119.
[9] Garcia-Martinez, H. A.; Llamas-Bueno, M.; Song, S.; Lopez-Valdivieso, A. Computational Study on Stability of Magnetite and Quartz Suspensions in an External Magnetic Field. *J. Dispers. Sci. Technol.* **2005**, *26* (2), 177–182.
[10] ZHANG, P.; Qiang, Z. H. U.; Qian, S. U.; Bin, G. U. O.; CHENG, S. Corrosion Behavior of T2 Copper in 3.5% Sodium Chloride Solution Treated by Rotating Electromagnetic Field. *Trans. Nonferrous Met. Soc. China* **2016**, *26* (5), 1439–1446.
[11] LI, J.; ZHANG, P.; Bin, G. U. O. Effects of Rotating Electromagnetic on Flow Corrosion of Copper in Seawater. *Trans. Nonferrous Met. Soc. China* **2011**, *21*, s489–s493.
[12] Zhang, P.; Guo, B.; Jin, Y.-P.; Cheng, S.-K. Corrosion Characteristics of Copper in Magnetized Sea Water. *Trans. Nonferrous Met. Soc. China* **2007**, *17* (s1A), s189–s193.
[13] Bikul'chyus, G.; Ruchinskene, A.; Deninis, V. Corrosion Behavior of Low-Carbon Steel in Tap Water Treated with Permanent Magnetic Field. *Prot. Met.* **2003**, *39* (5), 443–447.
[14] Hryniewicz, T.; Rokosz, K.; Rokicki, R. Electrochemical and XPS Studies of AISI 316L Stainless Steel after Electropolishing in a Magnetic Field. *Corros. Sci.* **2008**, *50* (9), 2676–2681.
[15] Chiba, A.; Kawazu, K.; Nakano, O.; Tamura, T.; Yoshihara, S.; Sato, E. The Effects of Magnetic Fields on the Corrosion of Aluminum Foil in Sodium Chloride Solutions. *Corros. Sci.* **1994**, *36* (3), 539–543.
[16] Jayaraman, T. V; Guruswamy, S.; Free, M. L. Effect of Magnetic Field on the Corrosion Behavior of Magnetostrictive Iron-Gallium Alloy Single Crystals. *Corrosion* **2007**, *63* (11), 1042–1047.
[17] Li, J.; Zhang, T.; Shao, Y.; Meng, G.; Wang, F. A Stochastic Analysis of the Effect of Magnetic Field on the Pitting Corrosion Susceptibility of Pure Magnesium. *Mater. Corros.* **2010**, *61* (4), 306–312.
[18] Ghabashy, M. E.; Sedahmed, G. H.; Mansour, I. A. S. Effect of a Magnetic Field on the Rate of Diffusion-Controlled Corrosion of Metals. *Br. Corros. J.* **2013**.
[19] Shinohara, K.; Aogaki, R. Magnetic Field Effect on Copper Corrosion in Nitric Acid. *Denki Kagaku Oyobi Kogyo Butsuri Kagaku* **1999**, *67* (2), 126–131.
[20] Chiba, A.; Okada, M.; Ogawa, T. Magnetic Field Effects on Dissolution of Nickel, Copper, Zinc and Brass in Nitric Acid Solution. *Boshoku Gijutsu(Corros. Eng.)* **1988**, *37* (5), 259–264.
[21] Busch, K. W.; Busch, M. A.; Parker, D. H.; Darling, R. E.; McAtee Jr, J. L. Studies of a Water Treatment Device That Uses Magnetic Fields. *Corrosion* **1986**, *42* (4), 211–221.
[22] Sagawa, M. Effect of a Local Magnetic Field on the Dissolution of Copper and Iron in Nitric Acid Solution. *Trans. Japan Inst. Met.* **1982**, *23* (1), 38–40.
[23] Sueptitz, R.; Tschulik, K.; Uhlemann, M.; Eckert, J.; Gebert, A. Retarding the Corrosion of Iron by Inhomogeneous Magnetic Fields. *Mater. Corros.* **2014**, *65* (8), 803–808.
[24] Chiba, A.; Tanaka, N.; Ueno, S.; Ogawa, T. Inhibition of Iron Corrosion in Sodium Chloride Solutions by Magnetic Fields. *Corros. Eng.* **1992**, *45* (5), 333–341.
[25] Ručinskien, A.; Bikulčius, G.; Gudavičiūt, L.; Juzeliūnas, E. Magnetic Field Effect on Stainless Steel Corrosion in FeCl 3 Solution. *Electrochem. commun.* **2002**, *4* (1), 86–91.
[26] Srivastava, K.; Nigam, N. Protection of Mild Steel in Sulphuric Acid by Magnetic Fields. *Br. Corros. J.* **2013**.
[27] Chiba, A.; Ogawa, T. Effects of Magnetic Field Direction on the Dissolution of Copper, Zinc, and Brass in Nitric Acid [J]. *Corros. Eng* **1988**, *37* (10), 531.
[28] Gokhale, S.; Ellis, S. API Specification 5CT N-80 Grade Casing May Burst or Part Unexpectedly If Supplementary Metallurgical Requirements Are Not Specified. Society of Petroleum Engineers.
[29] Farshad, F. F.; Linsley, J.; Kuznetsov, O.; Vargas, S. The Effects of Magnetic Treatment on Calcium Sulfate Scale Formation. In *SPE Western Regional/AAPG Pacific Section Joint Meeting*; Society of Petroleum Engineers, 2002.
[30] İlbay, Z.; Şahin, S.; Büyükkabasakal, K. A Novel Approach for Olive Leaf Extraction through Ultrasound Technology: Response Surface Methodology versus Artificial Neural Networks. *Korean J. Chem. Eng.* **2014**, *31* (9), 1661–1667.
[31] Mansouri, Y.; Zinatizadeh, A. A.; Mohammadi, P.; Irandoust, M.; Akhbari, A.; Davoodi, R. Hydraulic Characteristics Analysis of an Anaerobic Rotatory Biological Contactor (AnRBC) Using Tracer Experiments and Response Surface Methodology (RSM). *Korean J. Chem. Eng.* **2012**, *29* (7), 891–902.
[32] Karmakar, M.; Mahapatra, M.; Singha, N. R. Separation of Tetrahydrofuran Using RSM Optimized Accelerator-Sulfur-Filler of Rubber Membranes: Systematic Optimization and Comprehensive Mechanistic Study. *Korean J. Chem. Eng.* **2017**, *34* (5), 1416–1434.
[33] Suwanthai, W.; Punsuvon, V.; Vaithanomsat, P. Optimization of Biodiesel Production from a Calcium Methoxide Catalyst Using a Statistical Model. *Korean J. Chem. Eng.* **2016**, *33* (1), 90–98.
[34] Tak, K.; Kim, J.; Kwon, H.; Cho, J. H.; Moon, I. Kriging Models for Forecasting Crude Unit Overhead Corrosion. *Korean J. Chem. Eng.* **2016**, *33* (7), 1999–2006.
[35] Noor, E. A.; Al-Moubaraki, A. H. Corrosion Behavior of Mild Steel in Hydrochloric Acid Solutions. *Int. J. Electrochem. Sci* **2008**, *3* (1), 806–818.
[36] Chin, R. J.; Nobe, K. Electrodissolution Kinetics of Iron in Chloride Solutions III. Acidic Solutions. *J. Electrochem. Soc.* **1972**, *119* (11), 1457–1461.
[37] MacFarlane, D. R.; Smedley, S. I. The Dissolution Mechanism of Iron in Chloride Solutions. *J. Electrochem. Soc.* **1986**, *133* (11), 2240–2244.
[38] Uhlig, H. H.; King, C. V. Corrosion and Corrosion Control. *J. Electrochem. Soc.* **1972**, *119* (12), 327C–327C.
[39] Ashassi-Sorkhabi, H.; Seifzadeh, D. The Inhibition of Steel Corrosion in Hydrochloric Acid Solution by Juice of Prunus Cerasus. *Int. J. Electrochem. Sci* **2006**, *1* (1), 92–96.
[40] Imamura, T.; Yamada, Y.; Oi, S.; Honda, H. Orientation Behavior of Carbonaceous Mesophase Spherules Having a New Molecular Arrangement in a Magnetic Field. *Carbon N. Y.* **1978**, *16* (6), 481–486.
[41] Chang, K.-T.; Weng, C.-I. The Effect of an External Magnetic Field on the Structure of Liquid Water Using Molecular Dynamics Simulation. *J. Appl. Phys.* **2006**, *100* (4), 43917.
[42] Cai, R.; Yang, H.; He, J.; Zhu, W. The Effects of Magnetic

Fields on Water Molecular Hydrogen Bonds. *J. Mol. Struct.* **2009**, *938* (1), 15–19.

[43] Moosavi, F.; Gholizadeh, M. Magnetic Effects on the Solvent Properties Investigated by Molecular Dynamics Simulation. *J. Magn. Magn. Mater.* **2014**, *354*, 239–247.

[44] Hosoda, H.; Mori, H.; Sogoshi, N.; Nagasawa, A.; Nakabayashi, S. Refractive Indices of Water and Aqueous Electrolyte Solutions under High Magnetic Fields. *J. Phys. Chem. A* **2004**, *108* (9), 1461–1464.

[45] Neufeld, P. Effect of Magnetic Fields on Electrochemical Reactions. *Corros. Sci.* **1994**, *36* (11), 1947–1948.

[46] Lu, Z.; Yang, W. In Situ Monitoring the Effects of a Magnetic Field on the Open-Circuit Corrosion States of Iron in Acidic and Neutral Solutions. *Corros. Sci.* **2008**, *50* (2), 510–522.

[47] Lu, Z.; Huang, C.; Huang, D.; Yang, W. Effects of a Magnetic Field on the Anodic Dissolution, Passivation and Transpassivation Behaviour of Iron in Weakly Alkaline Solutions with or without Halides. *Corros. Sci.* **2006**, *48* (10), 3049–3077.

[48] Linhardt, P.; Ball, G.; Schlemmer, E. Electrochemical Investigation of Chloride Induced Pitting of Stainless Steel under the Influence of a Magnetic Field. *Corros. Sci.* **2005**, *47* (7), 1599–1603.

[49] Sueptitz, R.; Koza, J.; Uhlemann, M.; Gebert, A.; Schultz, L. Magnetic Field Effect on the Anodic Behaviour of a Ferromagnetic Electrode in Acidic Solutions. *Electrochim. Acta* **2009**, *54* (8), 2229–2233.

[50] Tang, Y. C.; Davenport, A. J. Magnetic Field Effects on the Corrosion of Artificial Pit Electrodes and Pits in Thin Films. *J. Electrochem. Soc.* **2007**, *154* (7), C362–C370.

[51] Lu, Z.; Huang, D.; Yang, W.; Congleton, J. Effects of an Applied Magnetic Field on the Dissolution and Passivation of Iron in Sulphuric Acid. *Corros. Sci.* **2003**, *45* (10), 2233–2249.

[52] Yu, Q.-K.; Miyakita, Y.; Nakabayashi, S.; Baba, R. Magnetic Field Effect on Electrochemical Oscillations during Iron Dissolution. *Electrochem. commun.* **2003**, *5* (4), 321–324.

[53] Rhen, F. M. F.; Fernandez, D.; Hinds, G.; Coey, J. M. D. Influence of a Magnetic Field on the Electrochemical Rest Potential. *J. Electrochem. Soc.* **2006**, *153* (1), J1–J7.

[54] Lu, Z.; Huang, D.; Yang, W. Probing into the Effects of a Magnetic Field on the Electrode Processes of Iron in Sulphuric Acid Solutions with Dichromate Based on the Fundamental Electrochemistry Kinetics. *Corros. Sci.* **2005**, *47* (6), 1471–1492.

[55] Sueptitz, R.; Tschulik, K.; Uhlemann, M.; Schultz, L.; Gebert, A. Effect of High Gradient Magnetic Fields on the Anodic Behaviour and Localized Corrosion of Iron in Sulphuric Acid Solutions. *Corros. Sci.* **2011**, *53* (10), 3222–3230.

[56] Roy, R. K. *Design of Experiments Using the Taguchi Approach: 16 Steps to Product and Process Improvement*; John Wiley & Sons, 2001.

[57] Salehuddin, F.; Kaharudin, K. E.; Zain, A. S. M.; Yamin, A. K. M.; Ahmad, I. Analysis of Process Parameter Effect on DIBL in N-Channel MOSFET Device Using L27 Orthogonal Array. In *3RD INTERNATIONAL CONFERENCE ON FUNDAMENTAL AND APPLIED SCIENCES (ICFAS 2014): Innovative Research in Applied Sciences for a Sustainable Future*; AIP Publishing, 2014; Vol. 1621, pp 322–328.

[58] Inaba, H.; Saitou, T.; Tozaki, K.; Hayashi, H. Effect of the Magnetic Field on the Melting Transition of H2O and D2O Measured by a High Resolution and Supersensitive Differential Scanning Calorimeter. *J. Appl. Phys.* **2004**, *96* (11), 6127–6132.

[59] Higashitani, K.; Kage, A.; Katamura, S.; Imai, K.; Hatade, S. Effects of a Magnetic Field on the Formation of CaCO 3 Particles. *J. Colloid Interface Sci.* **1993**, *156* (1), 90–95.

[60] Baker, J. S.; Judd, S. J. Magnetic Amelioration of Scale Formation. *Water Res.* **1996**, *30* (2), 247–260.

نشریه فناوری نفت، گاز و پتروشیمی، ۸(۲): ۱-۱۳، تابستان و پاییز ۱۳۹۹

مقاله تحقیقاتی

مطالعه آزمایشگاهی و مدلسازی تأثیر میدان مغناطیسی القایی متغیر بر خوردگی لوله جداری چاه‌های نفت و گاز در عملیات اسیدکاری ماتریسی هیدروکلرویک اسید

عباس هاشمی‌زاده [۱،*]، محمدجواد عامری [۲]، بایک امین شهیدی [۳]، مصطفی قلی زاده [۴]

۱. گروه مهندسی شیمی، دانشکده فنی مهندسی، دانشگاه قم

۲. گروه مهندسی نفت، دانشکده مهندسی نفت، دانشگاه صنعتی امیرکبیر

۳. گروه مهندسی نفت، دانشکده فنی، دانشگاه فردوسی مشهد

۴. گروه شیمی آلی، دانشکده علوم پایه، دانشگاه فردوسی مشهد

مشخصات مقاله

تاریخچه مقاله:

دریافت: ۲۸ اردیبهشت ۱۴۰۰

دریافت پس از اصلاح: ۱۷ شهریور ۱۴۰۰

پذیرش نهایی: ۱۹ شهریور ۱۴۰۰

کلمات کلیدی:

اسیدکاری ماتریسی،

لوله جداری،

نرخ خوردگی،

مدلسازی،

پاسخ سطح

* عهده‌دار مکاتبات؛

رایانامه: a.hashemizadeh@hsu.ac.ir

تلفن: ۰۵۱-۴۴۰۱۲۸۵۹

دورنگار: ۰۵۱-۴۴۰۱۲۸۵۳

چکیده

اثر یک میدان مغناطیسی (MF) متغیر بر میزان خوردگی فولاد کربنی N-80 (که در صنعت نفت از جلمه لوله جداری چاه‌های نفت و گاز کاربرد زیادی دارد) در محلول HCl 12.5 درصد وزنی (۸،۳ مولار) برای اولین بار در شرایط مختلف با استفاده از روش‌های کاهش وزن (WL) و قطبش پتانسیودینامیک (PDP) اندازه‌گیری شد. برای بررسی و مدل سازی اثرات شدت میدان مغناطیسی، زمان مغناطیسی شدن و زمان سپری شده بر بازده جلوگیری از خوردگی (η)، از روش پاسخ سطح (طرح Box-Behnken) استفاده شده است. نتایج تجربی نشان می دهد که اسید مغناطیسی سرعت خوردگی N-80 CS در HCl غلیظ را تا ۳۹٪ به شدت کاهش می‌دهد. بنابراین می‌توان از آن به عنوان یک گزینه مقرون به صرفه و سازگار با محیط زیست برای بازدارنده‌های خوردگی معمولی استفاده کرد. نتایج نشان داد که η با افزایش شدت میدان مغناطیسی افزایش می‌یابد. مورفولوژی سطح فولاد کربن N-80 با استفاده از SEM هم در محلول های HCl نرمال و هم مغناطیسی مورد بررسی قرار گرفت.

نحوه استناد به این مقاله:

Hashemizadeh A., Ameri MJ., Aminshahidy B, Gholizadeh M, The variable external magnetic field effect on corrosion behavior of drilling casing of oil and gas wells in matrix acidizing with HCl solution: Experimental study and modelling, Journal of Oil, Gas and Petrochemical Technology, 2021; 8(2): 1-13. DOI:110.22034/jogpt.2021.269918.1090.